

DOI: 10.1002/adma.200702334

Dynamic Imaging of Functionalized Multi-Walled Carbon Nanotube Systemic Circulation and Urinary Excretion**

By Lara Lacerda, Anuradha Soundararajan, Ravi Singh, Giorgia Pastorin, Khuloud T. Al-Jamal, John Turton, Peter Frederik, Maria A. Herrero, Shouping Li, Ande Bao, Dimitris Emfietzoglou, Stephen Mather, William T. Phillips, Maurizio Prato, Alberto Bianco, Beth Goins, and Kostas Kostarelos*

Intravenously administered, multi-walled carbon nanotubes functionalized with diethylenetriaminepentaacetic dianhydride (DTPA-MWNT) and radiolabeled with Indium-111 (^{111}In), were dynamically tracked in vivo using a microSingle Photon Emission Tomography (microSPECT) scanner. Imaging showed that nanotubes enter the systemic blood circulation and within

5 min begin to permeate through the renal glomerular filtration system into the bladder. Urinary excretion of DTPA-MWNT was confirmed at 24 h post-administration. The renal clearance of DTPA-MWNT in rats reported here opens the door to the use of MWNT as components of multiple diagnostic and therapeutic modalities in development for systemic indications such as cardiovascular diseases and cancer.

There has been an explosive increase in the number of nanomaterials designed for biomedical applications that has generated extraordinary interest and expectations for effective, disease-eradicating therapeutic modalities.^[1] At the same time, the toxicological burden and the pharmacological viability of such novel nanomaterials remain largely unknown, further complicating the discussion for the need of a new regulatory framework for nanomaterials.^[2] One such type of highly innovative nanomaterials is the CNT, first reported in the early 1990s by Iijima.^[3] Extraordinary characteristics of this material, consisting only of a network of carbon atoms in the nanometer scale, include great tensile strength, as well as high electrical and thermal conductivity.^[4]

Our work has focused on the pharmacological development of functionalized CNT (*f*-CNT) using the 1,3-dipolar cycloaddition reaction^[5] to render the CNT surfaces water-soluble and therefore compatible with the biological milieu. Various biomedical applications of *f*-CNT have been explored and encouraging proof-of-principle studies have indicated their effective role as delivery systems for genes, peptides, antimicrobial agents and cytotoxic drug molecules.^[6] However, the clinical evaluation of any therapeutic or diagnostic agent based on *f*-CNT will involve the administration or implantation of nanotubes and their matrices into patients. In order to design such clinical studies, preclinical development of *f*-CNT is essential, particularly the determination of their in vivo pharmacological profiles. Towards that goal we first reported tissue biodistribution and blood circulation half-life data following intravenous administration of single-walled CNT (SWNT) covalently functionalized with tracer radionuclides.^[7] Other laboratories have also carried out similar in vivo studies following intraperitoneal,^[8] intratumoral^[9] or intravenous^[10] administration of different types of CNT. A very recent report^[11] using the functionalization chemistry developed in our laboratories to conjugate monoclonal antibodies for tumor cell targeting of SWNT, also reported rapid, high levels of elimination of the nanotubes, in good agreement with our original observations.^[7] However, none of these reports elucidated the

[*] Prof. K. Kostarelos, L. Lacerda, R. Singh, Dr. K. T. Al-Jamal, Dr. J. Turton
Nanomedicine Laboratory, Centre for Drug Delivery Research
The School of Pharmacy, University of London
29-39 Brunswick Square, London WC1N 1AX (UK)
E-mail: kostas.kostarelos@pharmacy.ac.uk
A. Soundararajan, Dr. A. Bao, Prof. W. T. Phillips, Prof. B. Goins
Department of Radiology, University of Texas
Health Science Center at San Antonio
San Antonio TX (USA)
Dr. G. Pastorin, Dr. S. Li, Dr. A. Bianco
CNRS, Institut de Biologie Moléculaire et Cellulaire
Laboratoire d'Immunologie et Chimie Thérapeutiques
Strasbourg (France)
Dr. P. Frederik
Electron Microscopy Unit
School of Medicine, University of Maastricht
Maastricht (The Netherlands)
Dr. M. A. Herrero, Prof. M. Prato
Dipartimento di Scienze Farmaceutiche, Università di Trieste
Trieste (Italy)
Dr. D. Emfietzoglou
Department of Medical Physics, The School of Medicine, University
of Ioannina
Ioannina (Greece)
Prof. S. Mather
Nuclear Medicine Research Laboratory, St. Bartholomew's Hospital
London (UK)

[**] This work was supported by The School of Pharmacy, University of London and the United Kingdom Department and Trade & Industry (DTI) 'UK-Texas Collaborative Initiative' programme (grant QCBB/013/00057), the CNRS and the Agence Nationale de la Recherche (grant ANR-05-JCJC-0031-01), the University of Trieste and Italian MUR (PRIN 2006, prot.2006034372). L. L. acknowledges support by the Portuguese Foundation for Science and Technology (FCT/MCES) for the award of a PhD fellowship (Ref.: SFRH/BD/21845/2005). G. P. is grateful to French Ministry for Research and New Technologies for a post-doctoral fellowship (GenHomme Network 2003). This work was also supported by the European Union, NEURONANO program (NMP4-CT-2006-031847). TEM images were collected at the Microscopy Facility Platform of Esplanade Campus (IBMP, Strasbourg, France). The authors would also like to thank J. Sumner, UTHSCSA Radiology Department, for preparation of the figures of gamma camera images. Supporting Information is available online from Wiley InterScience or from the authors.

crucially important mechanism of elimination of the CNT from the tissues that CNT traversed or accumulated. Furthermore, no previous study has reported pharmacological data following intravenous administration of MWNT.

In order to determine the tissue distribution of functionalized MWNT, we have covalently attached onto the nanotube surface one of the most clinically established chelating molecule DTPA (Fig. 1a), which was subsequently used to cage the γ -emitting radionuclide ^{111}In as previously reported.^[7] The structural characteristics of MWNT before and after functionalization, were studied by transmission electron microscopy (TEM) indicating that the nanotubes were predominantly individualized, with average dimensions of 20–30 nm in diameter and few hundreds nm in length (Fig. 1b and c, for more detailed characterization information of MWNT please see Supporting Information). The resultant DTPA-MWNT were then reacted with $^{111}\text{InCl}_3$ to form the radio-conjugate (Fig. 2a). The labeling reaction yield was above 80 % as verified by TLC (Fig. 2b and c). Furthermore, the ^{111}In -labelled DTPA-MWNT construct (^{111}In]DTPA-MWNT) was shown to be stable following incubation in serum at 37 °C for 1 and 24 h (Fig. 2d and e).

Following the administration by tail vein injection of ^{111}In]DTPA-MWNT [300 μg of MWNT; 250 μCi (9.25 MBq) of ^{111}In] in rats, the animals were placed in a microSPECT/computed tomography (CT) unit and the dynamic tissue distribution of the radioactive nanotube conjugate was monitored and recorded. Figure 3a shows representative whole-body dynamic anterior planar gamma camera images of ^{111}In]DTPA-MWNT at the early post-administration time points of 0, 30, 60, 180, and 300 s (see also Supporting Video

for a compiled dynamic clip). As can be seen, the ^{111}In]DTPA-MWNT entered the systemic blood circulation and within 60 s began accumulating in the kidneys and bladder. Anterior planar gamma camera imaging (Fig. 3b) at 30 min, 6 h and 24 h post ^{111}In]DTPA-MWNT administration was subsequently carried out. Between imaging sessions, animals were maintained in metabolic cages and urine was collected for the duration of the imaging schedule. Within 30 min following ^{111}In]DTPA-MWNT administration, most of the observed radioactivity was localized in the kidneys and bladder. At 6 h almost all ^{111}In]DTPA-MWNT had been eliminated from the body via the renal excretion route. At 24 h only residual radioactivity levels were detected in the kidneys. This was also confirmed by the quantitative radioactivity analysis of harvested tissues at 24 h (Fig. 3c). Notably the % injected dose (% ID) per gram tissue of radioactivity detected in the urine within 24 h was more than a factor of 10 higher than the kidney values, the second highest, whereas almost no radioactivity was detected in lungs and reticuloendothelial system organs (liver and spleen).

Next, we investigated the histological impact of non-radiolabeled DTPA-MWNT as it traversed through the systemic circulation and the renal excretion route in comparison to non-functionalized, purified MWNT (pMWNT). Several studies^[12] have recently reported the effect of purified CNT (pCNT) administration in vivo, following local administration via the tracheal, nasal or subcutaneous routes. Most of these studies reported organ accumulation of pCNT. The intravenous administration of non-functionalized SWNT coated with block copolymer molecules (Pluronic F108) has been shown

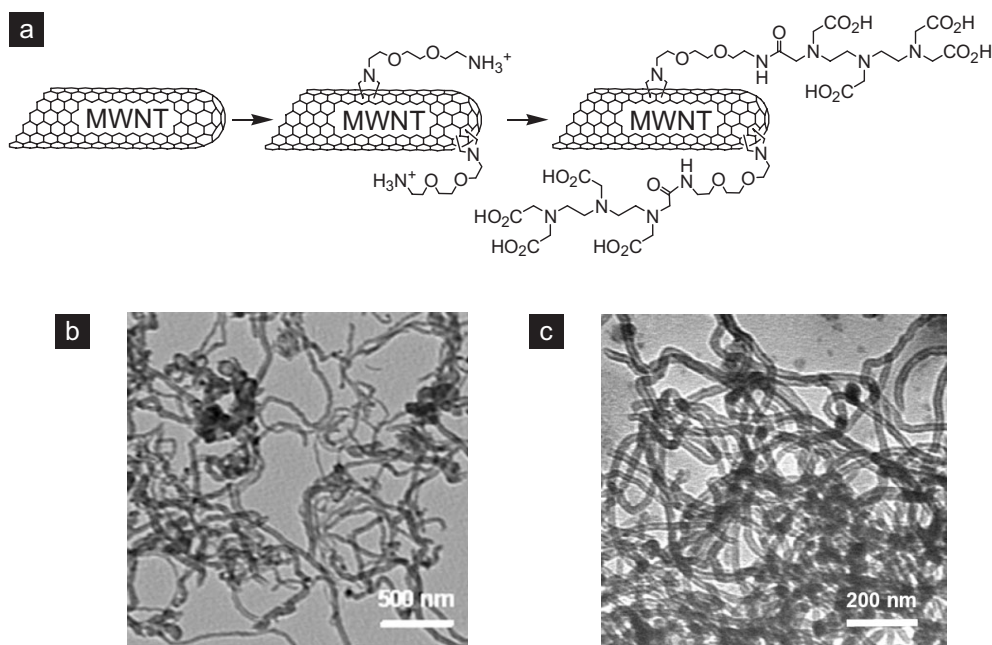


Figure 1. Structures of MWNT. a) Molecular structures of pMWNT, MWNT-NH₃⁺ and DTPA-MWNT (simplified structures depicting only outer nanotube cylinder are drawn); b) TEM images of pMWNT, and c) DTPA-MWNT. The nanotubes were suspended in an organic solvent (pMWNT) or water (DTPA-MWNT) before preparing the TEM grids. The TEM images clearly show the presence of concentric cylindrical structures typical of MWNT.

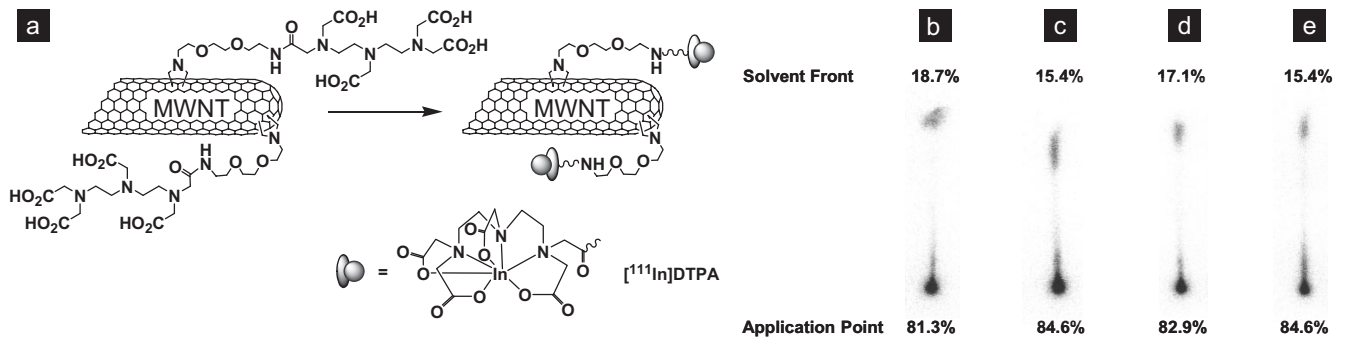


Figure 2. Serum stability of $[^{111}\text{In}]$ DTPA-MWNT conjugate. a) Molecular structures of DTPA-MWNT (left) and $[^{111}\text{In}]$ DTPA-MWNT (right) are shown. Images of the TLC strips after the labeling reaction and dilution of the $[^{111}\text{In}]$ DTPA-MWNT in a) PBS or b) serum. TLC strips of the $[^{111}\text{In}]$ DTPA-MWNT conjugates diluted in serum and incubated at 37°C for d) 1 h and e) 24 h.

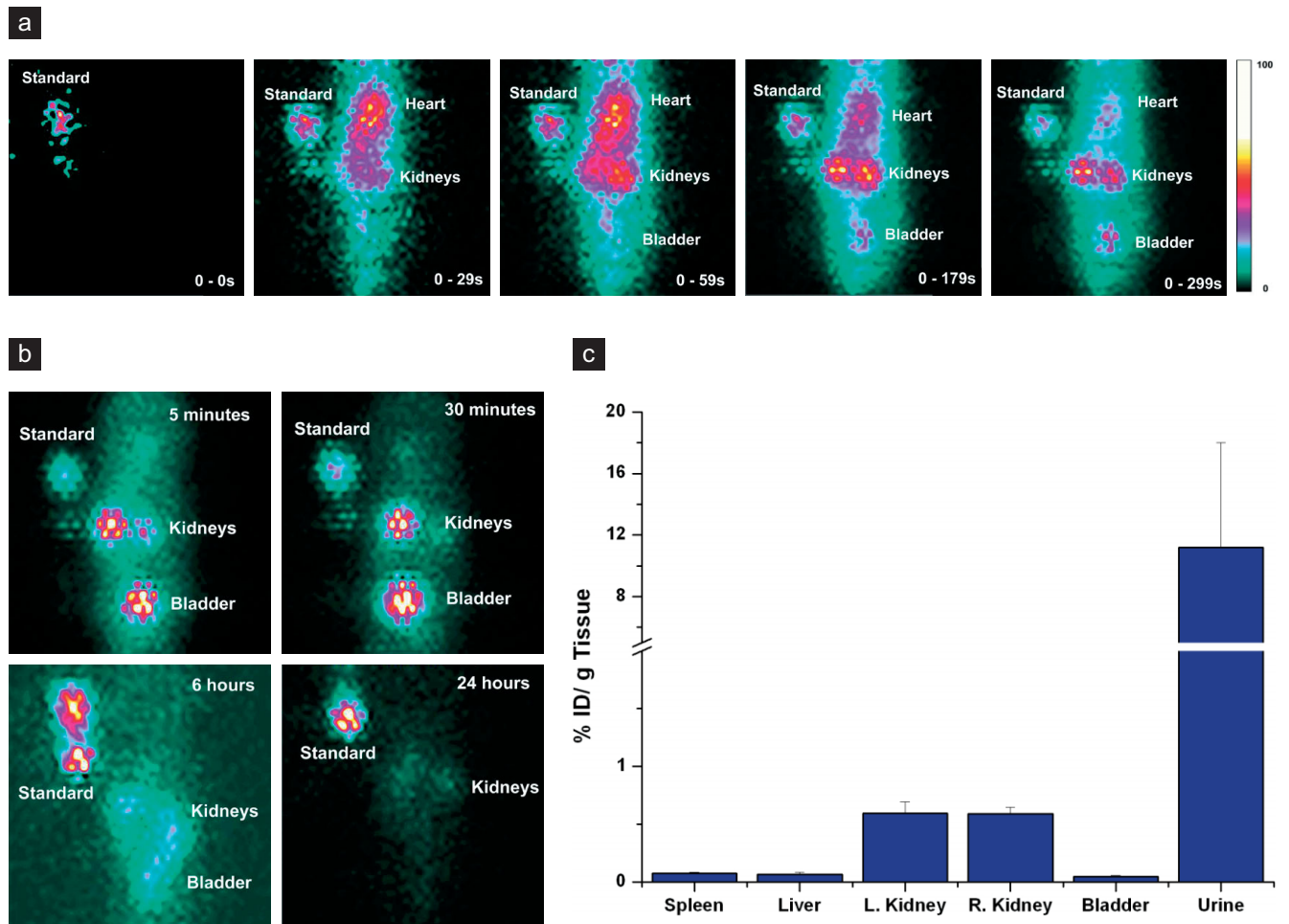


Figure 3. Normal rat distribution of $[^{111}\text{In}]$ DTPA-MWNT. a) Dynamic anterior planar images of whole body distribution of $[^{111}\text{In}]$ DTPA-MWNT within 5 min after intravenous administration in rats. Color scale for radioactivity levels shown in arbitrary units (see also Supporting Video online for a dynamic reconstruction). b) Static anterior planar images of whole body distribution of $[^{111}\text{In}]$ DTPA-MWNT in rats after 5 min, 30 min, 6 h, and 24 h post-injection (difference between Fig. 3a, 0–299 s image and Fig. 3b, 5 min image is due to lag-time in camera setup). c) % ID radioactivity per gram tissue at 24 h after intravenous administration of $[^{111}\text{In}]$ DTPA-MWNT quantified by gamma counting ($n = 3$ and error bars for standard deviation).

to lead to rapid clearance from systemic blood circulation and accumulation primarily in the liver.^[10a] For the purposes of this study, pMWNT were dispersed in aqueous media by coating with biological macromolecules (serum proteins) as described by others,^[13] by pre-incubation of nanotubes with serum prepared from the control animals of the same species and age, prior to intravenous administration. Non-radiolabeled DTPA-MWNT dispersions in phosphate buffered saline (PBS) and serum-coated pMWNT were injected via the tail vein in rats (600 µg of MWNT per rat) anesthetized with isoflurane. 24 h post-administration, the animals were sacrificed and the kidneys, liver, spleen, heart and lungs were harvested. Histological examination of rat tissues 24 h post MWNT administration, using hematoxylin and eosin stained sections, indicated that the lung (Fig. 4a and g) and liver (Fig. 4c and h)

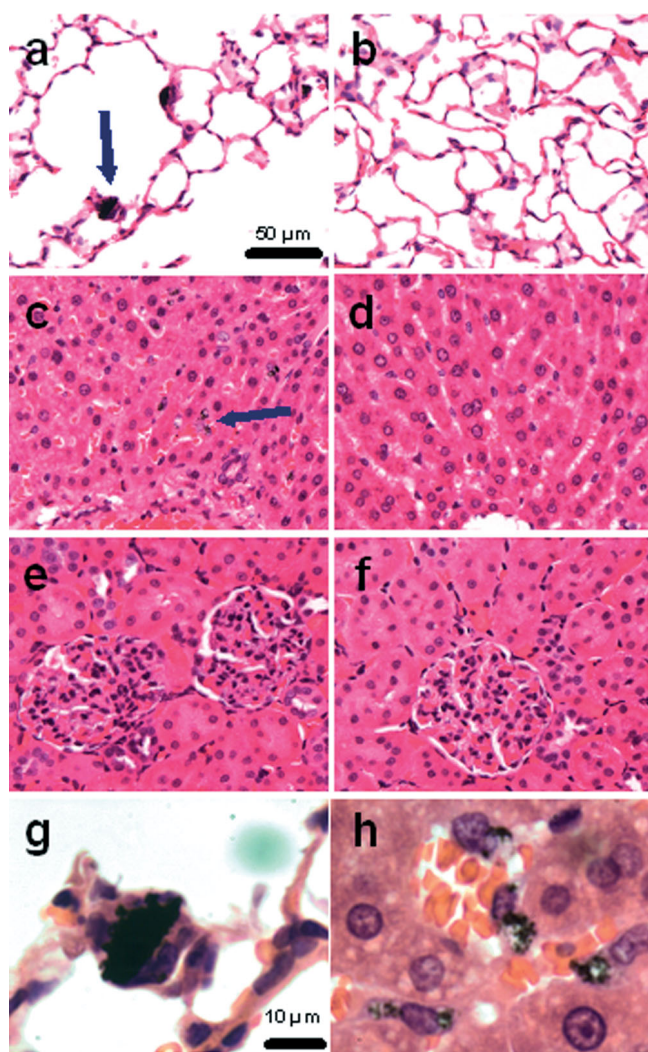


Figure 4. Histology of rat tissues. Hematoxylin and eosin stained sections of Wistar rat lung (a and b), liver (c and d), and kidney (e and f) at 24 h post-administration of 600 µg of pMWNT (a, c, and e) and 600 µg of DTPA-MWNT (b, d, and f). 20 x magnification for a–f. Arrows point to pMWNT aggregates accumulated in lung and liver which can be seen at higher magnification in g and h (80 x), respectively.

sections of animals that received pMWNT exhibited accumulation of dark pMWNT clusters. In the liver, Kupfer cells in the sinusoidal walls are observed to contain accumulated pMWNT (Fig. 4h). Very interestingly, intravenously administered DTPA-MWNT did not show any evidence of lung or liver accumulation, confirming our biodistribution data (Fig. 2).

Moreover, kidney histology for all groups (Fig. 4e and f) revealed normal renal morphology, without any MWNT accumulation. The data reported in this study show that covalently functionalized DTPA-MWNT can enter systemic blood circulation almost immediately upon tail vein injection in living animals. The rapid urinary clearance of intravenously administered DTPA-MWNT is in contrast to studies using non-covalently functionalized CNT that reported rapid blood clearance profiles predominantly leading to hepatic accumulation. The proposed mechanism of elimination is due to rapid desorption in blood of the macromolecules used to coat the CNT surface leading to bundles of circulating non-functionalized CNT accumulating in the liver tissue. Moreover, very recent studies^[14] reported that intraperitoneal administration of functionalized MWNT (functionalized by carboxylation and subsequent glucosamine conjugation) led to rapid and overwhelming excretion into the feces and urine.

The mechanism of DTPA-MWNT clearance through the glomerular filtration system seems to be devoid of significant residual nanotubes deposits in the kidney. Because the length of DTPA-MWNT used in this study is considerably larger than the dimensions of the glomerular capillary wall (minimum diameter of fenestra is 30 nm; thickness of the glomerular basement membrane in rats and humans is 200–400 nm; and width of the epithelial podocyte filtration slits is 40 nm),^[15] the longitudinal nanotube dimension does not appear to be a critical parameter in renal clearance as schematically depicted in Figure 5. The mechanism by which nanotubes pass through the glomerular filtration system must involve the acquisition of a molecular conformation in which the longitudinal DTPA-MWNT dimension is perpendicular to the glomerular fenestrations, since only the traverse dimension of DTPA-MWNT (cross-section is between 20–30 nm) is small enough to allow permeation through the glomerular pores.^[16] This suggests that DTPA-MWNT are ultra-deformable while in blood circulation, capable of reorientation when they reach the glomerular filtration system and able to readily pass into Bowman's space and subsequently the bladder. Moreover, recent reports have experimentally described water flow rates through CNT orders of magnitude faster than would be predicted from conventional hydrodynamics theory due to the almost frictionless water-carbon backbone interface.^[17] Such unique CNT properties are also thought to contribute towards the considerable glomerular hyperpermeability observed in our studies particularly in view of the hydraulic permeability and resistance properties of the glomerular capillary wall.^[18]

In the last few years, CNT have been intensively explored for a variety of biomedical applications. The determination of the pharmacological profiles of such carbon nanomaterials will have a determinant role in their transformation into clinically viable and effective therapeutics. It is now becom-

ing established knowledge that covalent functionalization, irrespective of functional group and chemistry, offers significant improvements in the toxicity profile of CNT *in vitro*^[19] and *in vivo*.^[20] More systematic investigations need to be carried out though, to determine the importance of CNT chemical structure on their interactions with biological milieu.

Systematic toxicological investigations are also now imperative, in order to study the impact of such CNT behavior on the physiopathology of tissues interacting with these novel nanomaterials in the short and long term, identify the impact of CNT dose responses and assess the overall safety of CNT *in vivo* before any further clinical development can be envisaged.

Experimental

MWNT: Non-functionalized, purified MWNT (pMWNT) were purchased from Nanostructured & Amorphous Materials Inc. (Houston, USA). Regular pMWNT used in this study were 94 % pure, stock No. 1240XH. Outer average diameter was between 20 and 30 nm, and length between 0.5 and 2 μm . Water-soluble diethylenetriamine-pentaacetic-functionalized MWNT (DTPA-MWNT) were prepared as described in detail elsewhere [7]. The number of free amino groups remaining on the DTPA-MWNT was measured by the quantitative Kaiser test (Supporting Information Table S1 online). According to the ratio between the number of amino groups present and the amount of DTPA used, 55 % of amines remained unreacted. The complexation between the DTPA-MWNT and the radionuclide $^{111}\text{InCl}_3$ (GE Healthcare Radiopharmacy, San Antonio, TX, USA) was carried out according to the method described previously for SWNT [7]. The stability constant between DTPA and ^{111}In has been previously determined by others [21] to be 1.5×10^{29} and previous studies have demonstrated that the [^{111}In]DTPA complex exhibits a strong chelating effect in the presence of human serum [22]. PBS suspensions of the obtained [^{111}In]DTPA-MWNT were used for the distribution studies in rats.

Serum Stability Studies: DTPA-MWNT and DTPA alone were labeled with $^{111}\text{InCl}_3$ (1.85 MBq) in a solution of 0.2 M ammonium acetate pH 5.5. The labeling reaction was stopped after 10 min by addition of 0.1 M EDTA. $^{111}\text{InCl}_3$ alone, used as a control, was also subjected to the conditions of the labeling reaction. Aliquots of each final product were diluted 1/5 in PBS and then spotted in silica gel impregnated glass fiber sheets (PALL Life Sciences). The strips were developed with a mobile phase of 50 mM EDTA in 0.1 M ammonium acetate. The strips were allowed to dry, followed by development and quantitative autoradiography counting using a Cyclone phosphor detector (Packard). The stability of the conjugate [^{111}In]DTPA-MWNT was determined after incubation in serum (Sera Laboratories International Ltd., UK). Small aliquots of the final products were diluted 1/5 in serum (at 37 °C) and incubated for 0, 60 min and 24 h at 37 °C. The percentage of [^{111}In]DTPA-MWNT conjugate (immobile spot) and free ^{111}In or [^{111}In]DTPA (mobile spot) was evaluated by TLC performed as described above (Supporting Information Fig. S2 online).

Normal Rat Distribution of [^{111}In]DTPA-MWNT: 6 week old, male, nude rats (Harlan, Indianapolis, IN, USA) were anesthetized by inhalation with isoflurane (3 % in 100 % Oxygen). 0.8 ml of [^{111}In]DTPA-MWNT in PBS, containing 250 μCi (9.25 MBq) of ^{111}In and 300 μg of DTPA-MWNT, was administered to each rat by bolus injection through the tail vein. Dynamic planar images were acquired with dual gamma cameras housed in a microSPECT/CT scanner (Gamma Medica Ideas, Northridge, CA, USA). Images were acquired using medium energy, high sensitivity parallel hole collimators immediately following injection at an image capture rate of 1 frame per second

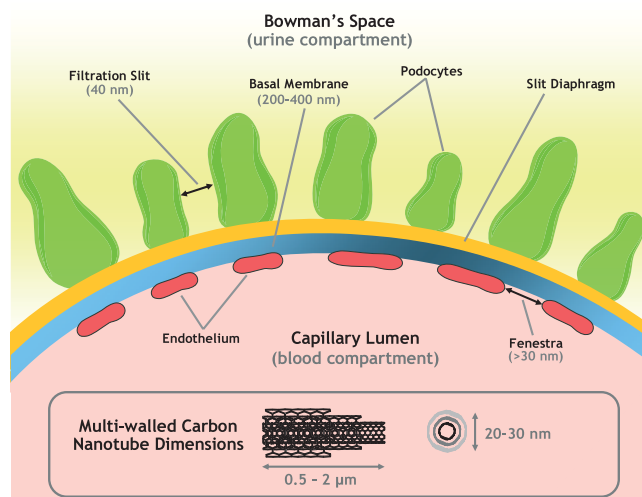


Figure 5. Schematic depiction of the principal components of the glomerular filtration system (top) compared to the longitudinal and traverse dimensions of a characteristic MWNT used in this study (boxed at the bottom).

during the first minute and 1 frame per 5 s for the following 4 min. Planar images were also acquired at 5 min, 30 min, 6 h, and 24 h post-injection. During each imaging session a standard [^{111}In]DTPA-MWNT source was positioned outside the animal but still within the field of view. The rats were placed individually in metabolic cages and sacrificed 24 h post-injection by cervical dislocation under deep isoflurane anesthesia. Bladder (with urine), both kidneys, liver, spleen and excreted urine were collected and placed into pre-weighed scintillation vials. Each organ was then weighed and samples were analysed for ^{111}In activity using an automated gamma counter (Wallac 1480 Wizard 3[™], Perkin Elmer Life Sciences, Boston, MA, USA). All procedures were performed according to the National Institutes of Health Animal Care and Use Guidelines and approved by the Institutional Animal Care Committee of the University of Texas Health Science Center at San Antonio.

Administration of MWNT and Histology of rat Tissues: Wistar rats were randomly separated in 4 groups and were intravenously injected by tail vein with 500 μl of PBS (PBS group, $n = 3$), 500 μl of PBS containing 600 μg of DTPA-MWNT (DTPA-MWNT group, $n = 4$), 500 μl of rat serum (serum group, $n = 3$), or 500 μl containing 600 μg of rat serum-coated pMWNT (pMWNT group, $n = 4$). This single dose of 600 μg of MWNT per rat represents the highest CNT dose ever intravenously injected in animals to date and was selected on the basis of our previous investigations describing construction of CNT-based gene delivery systems [6c]. Following administration of the MWNT, the rats were placed individually in metabolic cages (Tecniplast, UK). Urine production, water consumption and body weight were monitored over 24 h. The rats were sacrificed 24 h post-injection. The animals were necropsied and kidneys, liver, spleen, heart and lungs were harvested. These tissues were fixed in 10 % buffered formalin and processed for routine histology with hematoxylin and eosin stain by the Laboratory Diagnostic Service of the Royal Veterinary College (London, UK). Microscopic observation of tissues was carried out with a Nikon Microphot-FXA microscope coupled with a digital camera (Infinity 2).

Received: September 13, 2007
Published online: December 11, 2007

- [1] G. M. Whitesides, *Nat. Biotechnol.* **2003**, *21*, 1161.
[2] a) G. Brumfiel, *Nature* **2006**, *440*, 262. b) R. F. Service, *Science* **2005**, *309*, 36.

- [3] S. Iijima, *Nature* **1991**, 354, 56.
- [4] R. Saito, G. Dresselhaus, M. S. Dresselhaus, *Physical Properties of Carbon Nanotubes*, Imperial College Press, London **1998**.
- [5] V. Georgakilas, K. Kordatos, M. Prato, D. M. Guldi, M. Holzinger, A. Hirsch, *J. Am. Chem. Soc.* **2002**, 124, 760.
- [6] a) D. Pantarotto, C. D. Partidos, J. Hoebeke, F. Brown, E. Kramer, J.-P. Briand, S. Muller, M. Prato, A. Bianco, *Chem. Biol.* **2003**, 10, 961. b) D. Pantarotto, R. Singh, D. McCarthy, M. Erhardt, J. P. Briand, M. Prato, K. Kostarelos, A. Bianco, *Angew. Chem. Int. Ed.* **2004**, 43, 5242. c) R. Singh, D. Pantarotto, D. McCarthy, O. Chaloin, J. Hoebeke, C. D. Partidos, J. P. Briand, M. Prato, A. Bianco, K. Kostarelos, *J. Am. Chem. Soc.* **2005**, 127, 4388. d) W. Wu, S. Wieckowski, G. Pastorin, M. Benincasa, C. Klumpp, J. P. Briand, R. Gennaro, M. Prato, A. Bianco, *Angew. Chem. Int. Ed.* **2005**, 44, 6358. e) G. Pastorin, W. Wu, S. Wieckowski, J. P. Briand, K. Kostarelos, M. Prato, A. Bianco, *Chem. Commun.* **2006**, 1182.
- [7] R. Singh, D. Pantarotto, L. Lacerda, G. Pastorin, C. Klumpp, M. Prato, A. Bianco, K. Kostarelos, *Proc. Natl. Acad. Sci. USA* **2006**, 103, 3357.
- [8] H. F. Wang, J. Wang, X. Y. Deng, H. F. Sun, Z. J. Shi, Z. N. Gu, Y. F. Liu, Y. L. Zhao, *J. Nanosci. Nanotechnol.* **2004**, 4, 1019.
- [9] Z. Zhang, X. Yang, Y. Zhang, B. Zeng, S. Wang, T. Zhu, R. B. Roden, Y. Chen, R. Yang, *Clin. Cancer Res.* **2006**, 12, 4933.
- [10] a) P. Cherukuri, C. J. Gannon, T. K. Leeuw, H. K. Schmidt, R. E. Smalley, S. A. Curley, R. B. Weisman, *Proc. Natl. Acad. Sci. USA* **2006**, 103, 18882. b) Z. Liu, W. Cai, L. He, N. Nakayama, K. Chen, X. Sun, X. Chen, H. Dai, *Nat. Nanotechnol.* **2006**, 2, 47.
- [11] M. R. McDevitt, D. Chattopadhyay, B. J. Kappel, J. S. Jaggi, S. R. Schiffman, C. Antczak, J. T. Njardarson, R. Brentjens, D. A. Scheinberg, *J. Nucl. Med.* **2007**, 48, 1180.
- [12] L. Lacerda, A. Bianco, M. Prato, K. Kostarelos, *Adv. Drug Delivery Rev.* **2006**, 58, 1460.
- [13] C. W. Lam, J. T. James, R. McCluskey, R. L. Hunter, *Toxicol. Sci.* **2004**, 77, 126.
- [14] J. Guo, X. Zhang, Q. Li, W. Li, *Nucl. Med. Biol.* **2007**, 34, 579.
- [15] W. M. Deen, *J. Clin. Invest.* **2004**, 114, 1412.
- [16] a) W. M. Deen, M. J. Lazzara, B. D. Myers, *Am. J. Physiol. Renal Physiol.* **2001**, 281, F579. b) D. Venturoli, B. Rippe, *Am. J. Physiol. Renal Physiol.* **2005**, 288, F605.
- [17] a) M. Majumder, N. Chopra, R. Andrews, B. J. Hinds, *Nature* **2005**, 438, 44. b) J. K. Holt, H. G. Park, Y. Wang, M. Stadermann, A. B. Artyukhin, C. P. Grigoropoulos, A. Noy, O. Bakajin, *Science* **2006**, 312, 1034.
- [18] M. C. Drumond, W. M. Deen, *Am. J. Physiol.* **1994**, 266, F1.
- [19] C. M. Sayes, F. Liang, J. L. Hudson, J. Mendez, W. Guo, J. M. Beach, V. C. Moore, C. D. Doyle, J. L. West, W. E. Billups, K. D. Ausman, V. L. Colvin, *Toxicol. Lett.* **2006**, 161, 135.
- [20] J. C. Carrero-Sanchez, A. L. Elias, R. Mancilla, G. Arrellin, H. Terrones, J. P. Lacleite, M. Terrones, *Nano Lett.* **2006**, 6, 1609.
- [21] P. I. Ivanov, G. D. Bontchev, G. A. Bozhikov, D. V. Filossofov, O. D. Maslov, M. V. Milanov, S. N. Dmitriev, *Appl. Radiat. Isot.* **2003**, 58, 1.
- [22] F. Jasanada, P. Urizzi, J. P. Souchard, F. Le Gaillard, G. Favre, F. Nepveu, *Bioconjugate Chem.* **1996**, 7, 72.